Journal of Neurochemistry. 1962, Vol. 9, pp. 179 to 198. Pergamon Press Ltd. Printed in Northern Ireland

A MAPPING OF OXIDATIVE ENZYMES IN THE HUMAN BRAIN*

REINHARD L. FRIEDE and LADONA M. FLEMING
Mental Health Research Institute
University of Michigan, Ann Arbor, Michigan

(*Received* 2 *October* 1961)

THIS ARTICLE provides a quantitative mapping of the distribution of DPN-diaphorase activity in the nuclei and regions of the human brain. Measurements in fibre tracts were included although the article refers mainly to findings in grey matter; a detailed account of the enzyme pattern in white matter was published previously (FRIEDE, 1961*b*).

MATERIAL AND METHODS

Histochemical techniques. Six normal adult human brains from average post mortem material were used. They were placed in neutral 10% formalin 3–9 hr after death and fixed at 5° for 2 days. After 1-day fixation, the material was blocked into pieces 4–6 mm thick. Frozen sections were cut at 30 μ, rinsed in H_2O and incubated for 2 hr at 38° with frequent agitation. The method of FARBER, STERNBERG and DUNLAP (1956) was employed, using Nitro BT and tris buffer. Other techniques such as that of SCARPELLI, HESS and PEARSE (1958) and other tetrazolium salts had been used with identical results.† The pH of the incubation medium was always adjusted to 7·35. Sections from each block were incubated in individual jars and the proportion of incubation media to tissue was approximately the same for each. The reaction was stopped by transferring the sections to 10% neutral formalin. Half of the sections were mounted in glycerin gel; the others were dehydrated and mounted in Permount. Random material was used for the demonstration of succinic dehydrogenase (NACHLASS *et al.*, 1957) and cytochrome oxidase (BURSTONE, 1958) in 60 μ unfixed sections.

Quantitative techniques. For quantitative DPN-diaphorase determinations large series were used from three normal human brains. They were fixed and sectioned in the same way as sections used for histochemical studies. The incubation medium was the same except that the monotetrazolium salt INT was substituted for Nitro BT because Nitro BT formazan is very insoluble. The final concentration of tetrazolium salt in the incubation medium was 0·23 mg/ml for both the histochemical and quantitative studies. The sections were stored in chilled distilled H_2O until all the sections from one brain were cut. After all the sections were transferred to a beaker containing the buffer component of the incubation medium, they were gently poured into the rest of the incubation medium in a 2 l. Erlenmeyer flask which was shaken constantly in an Eberbach shaker-water bath at 38° for 2 hr. The reaction was stopped by transferring the entire contents of the flask into a large quantity of 10% formalin. The constant shaking increased the rate of the reaction and prevented uneven staining due to folded tissue. To make an accurate comparison of the amount of INT reduced formazan in all areas it was necessary completely to eliminate even minute variations in the time and temperature of fixation and incubation, in the degree of shaking and, particularly, in the proportion of tissue to incubation medium. Thus, all the sections from one brain were incubated in a single large quantity (600 ml) of incubation medium. When this is done, it is a reliable method for showing patterns within one specimen. It has been shown that the quantity of formazan formed is directly proportional to the enzyme activity (SHELTON and RICE, 1957). If the method was to be applied to experimental specimens, it was necessary to incubate sections from a control specimen in the same incubation bath each time. A 3 × 2 in. slide was covered with parafilm and each section was temporarily mounted on this to facilitate punching of small discs in the areas of interest. Sharpened stainless steel tubes, 1·1 mm and 2·4 mm in diameter were used to cut the discs. The INT formazan of each disc was extracted in 3 ml of 3:1 (v/v) ethanol–tetrachloroethylene (Eastman, Rochester, N.Y.). One drop of 1 N-HCl was added to each tube of extracted formazan, to ensure that the colour would be stable for

* This investigation was supported by U.S. Public Health Grant B3250.

† The reliabilityof these methods in formalin-fixed tissue has been tested extensively by comparison with assays in tissue homogenates; this data will be reported later.

several hours. The colour density was read at 500 mμ in a Beckman DU spectrophotometer and compared with standards prepared by dissolving weighed amounts of INT formazan (Synthetical Laboratories, Niles) in 3:1 ethanol tetrachlorethylene. The absorption curve of both the commercial INT formazan and that produced in the sections had a peak at 500 mμ. Controls without substrate were run for each area. The mean values obtained for all areas consistently ranged from 2·0 to 2·4 μg formazan. This was considered negligible and was not reported with the data. Control discs of a specific area from two 15 μ sections gave the same result as one disc from a 30 μ section. Thus, the results were independent of section thickness up to 30 μ.

The discs of the olivary and dentate nuclei were photographed before the formazan was extracted from them. The photomicrographs were measured planimetrically to determine the proportion of grey and white matter in each. By using this ratio and known values from adjacent discs of white matter, the formazan per 0·0434 mm³ was calculated for these nuclei.

RESULTS

Arrangement of data. Table 1 contains the results of about 2,400 measurements made in three human brains. Since the data for a given nucleus were in the same order in all the brains, the means refer to the collected data from all three brains; the number of measurements for any given nucleus was about the same in each brain. This pooling of data increased the standard deviation slightly but it provided an average, typical pattern of enzyme gradations among nuclei. Measurements in the nucleus anterior dorsalis thalami and the nucleus mammilaris were listed separately for case No. 2 because the data in these areas differed from those of cases Nos. 1 and 3.

Data previously obtained in a mapping of the cat brain (FRIEDE, 1961*c*) are included in Table 1 to facilitate comparison; they refer to densitometric measurements of the succinic dehydrogenase reaction in tissue sections and to counts of the capillarization of nuclei in the medulla oblongata of the cat; for further information, the histochemical atlas should be consulted.

The typical cytological details of enzyme distribution in the nuclei of the human brain are described in Table 2. Particular attention is focussed on the gradations of enzymic activity in the perikarya and the neuropil, and on the sharpness of the borders

TABLE 1. DISTRIBUTION OF DPN-DIAPHORASE IN THE BRAIN

Human brain		Cat brain	
Distribution of DPN-diaphorase		Succinic dehydrogenase	Capillarization
Nucleus*	μg Formazan/0·0434 mm³ tissue	Densitometric extinction units	x/22·5 mm capillaries/mm³ tissue
Medulla spinalis (cervical)			
Columna ventralis	33 ± 4		
Columna lateralis	35 ± 5		
Dorsomedial cell groups	30·5 ± 3		
Nucl. tractus spinalis trigemini	38·2 ± 6		
Nucl. gracilis (caudal part)	22·5 ± 3		
Tissue surrounding the canalis centralis	24·5 ± 3		
Ventral tracts	15·0 ± 3		
Lateral tracts	16·0 ± 2		
Dorsal tracts	12·0 ± 1		

* Anatomical names according to OLSZEWSKI and BAXTER (1954).

TABLE 1 (*cont'd*)

Human brain		Cat brain	
Distribution of DPN-diaphorase		Succinic dehydrogenase	Capillarization
Nucleus†	μg Formazan/0·0434 mm³ tissue	Densitometric extinction units	x/22·5 mm capillaries/mm³ tissue
Medulla oblongata			
Nucl. gracilis	30 ± 4	33 ± 5	32 ± 2
Nucl. cuneatus medialis	29 ± 4		
Nucl. cuneatus lateralis	44 ± 5	43 ± 7	46 ± 4
Nucl. tractus desc. n. trigemini			
(a) general region	31 ± 8		
(b) confined nucleus	39 ± 5	34 ± 3	32 ± 3
Nucl. n. hypoglossi	43 ± 5	46 ± 6	49 ± 5
Nucl. tractus solitarii	28 ± 4	16 ± 3	26 ± 3
Nucl. reticularis	30 ± 5	29 ± 4 37 ± 7	29 ± 2 32 ± 2
Nucl. reticularis lateralis	34 ± 6	41 ± 8*	41 ± 2
Nucl. olivaris	57 ± 9	53 ± 7	52 ± 10
Nucl. vestibularis medialis	43 ± 4	45 ± 5	44 ± 3
Nucl. vestibularis lateralis	33 ± 4	25 ± 4	35 ± 3
Tuberculum acousticum	47 ± 6	37 ± 6	52 ± 3
Nucl. prepositus hypoglossi	37 ± 8	35 ± 4	35 ± 3
Nucl. cochlearis	44	36 ± 6	43 ± 3
Nucl. arcuatus	51 ± 6		
Nucl. centralis medialis	42 ± 4		
Tractus pyramidalis	13 ± 2	8 ± 2	16 ± 2
Corpus restiforme	14 ± 2		
Cerebellum			
Stratum moleculare	33 ± 5		
Stratum granulare	32 ± 7		
Cortex (total)	34 ± 7		
Nucl. fastigii	46 ± 1		
Nucl. dentatus	55 ± 8		
Substantia alba	17 ± 2		
Pons			
Nucl. reticularis	25 ± 4	38 ± 5*	32 ± 2
Nucl. n. abducentis	34 ± 5		
Griseum centrale	23 ± 7	33 ± 5	31 ± 5
Nucl. supragenualis	22 ± 5		
Nucl. coeruleus	19 ± 1	21 ± 5	28 ± 2
Nucl. vestibularis superior	26 ± 3	32 ± 5*	34 ± 6
Nucl. vestibularis lateralis pars dorsalis	34 ± 5		
Nucl. n. trigemini motorius	39 ± 9		
Nucl. n. trigemini sensibilis	31 ± 11		
Nucl. parabrachialis	22 ± 3		
Nucl. parolivaris and nucl. olivaris superior	42 ± 7	59 ± 6* 59 ± 2*	56 ± 3 53 ± 3
Nucl. reticularis Bechterew (reticular part)	38 ± 3		

* Slightly higher densiometric data are marked by asterisk wherever it is felt that the spectrophotometric data include adjacent tissue with a weaker reaction.

† Anatomical names according to OLSZEWSKI and BAXTER (1954).

TABLE 1 (*cont'd*)

Human brain		Cat brain	
	Distribution of DPN-diaphorase	Succinic dehydrogenase	Capillarization
Nucleus†	μg Formazan/0·0434 mm³ tissue	Densitometric extinction units	x/22·5 mm capillaries/mm³ tissue
	Pons (cont.)		
Nucl. reticularis Bechterew (compact parts)	48 ± 5	45 ± 8	48 ± 4
Nucl. pontis (reticular part)	38 ± 2		
Nucl. pontis (compact part)	47 ± 3	41 ± 10	46 ± 5
Pyramidal tract	14 ± 3	8 ± 2	16 ± 2
Brachia pontis	13 ± 2		
Brachium conjunctivum	14 ± 2		
	Midbrain (colliculus inferior)		
Colliculus posterior (caudal part)	51 ± 3	66 ± 8*	51 ± 3
Colliculus posterior (cranial part)	37 ± 3		
Intercollicular region	30 ± 3		
Griseum centrale (dorsal portion)	32 ± 3	26 ± 4	26 ± 3
Griseum centrale (ventral portion)	17 ± 2	19 ± 3	20 ± 2
Area cuneiforme	23 ± 2	20 ± 4	26 ± 2
Nucl. trochlearis	43 ± 2	58 ± 7*	43 ± 4
Nucl. parabrachialis	25 ± 4	30 ± 6	28 ± 3
Lemniscus lateralis	11 ± 2		
Tractus pyramidalis	15 ± 3	8 ± 2	16 ± 2
	Midbrain (colliculus superior)		
Colliculus superior (lamina superficialis)	43 ± 3	64 ± 11*	50 ± 9
Colliculus superior (laminae profundae)	35 ± 4	36 ± 1	33 ± 2
Regio S	31 ± 4		
Griseum centrale (dorsolateral portion)	32 ± 6	42 ± 5	29 ± 3
Griseum centrale (ventromedial portion)	27 ± 4		
Dorsal crest (Nucl. dorsalis)	23 ± 2		
Pretectal area	30 ± 3		
Nucl. n. oculomotorii	51 ± 2	58 ± 7*	43 ± 4
Nucl. ruber (pars magnocellularis)	25 ± 3		
Nucl. ruber (transitional part)	31 ± 3		
Nucl. ruber (pars parvocellularis)	42 ± 7	43 ± 5	38 ± 3
Nucl. niger	26 ± 2	19 ± 3	30 ± 2
Pedunculi cerebri	15 ± 0	8 ± 2	16 ± 2

* Slightly higher densiometric data are marked by asterisk wherever it is felt that the spectrophotometric data include adjacent tissue with a weaker reaction.

† Anatomical names according to OLSZEWSKI and BAXTER (1954).

TABLE 1 (*cont'd*)

Human brain Distribution of DPN-diaphorase		Human brain Distribution of DPN-diaphorase	
Nucleus†	μg Formazan/0·0434 mm³ tissue	Nucleus†	μg Formazan/0·0434 mm³ tissue
	Diencephalon (thalamus)		
Nucl. anterior (dorsalis)		Midline-nuclear group	
Cases 1 & 3	45 ± 4	deep transition into hypothalamus	29 ± 4
Case 2	36 ± 2		
Nucl. lateralis pars anterior	34 ± 6		
Nucl. lateralis pars dorsalis	42 ± 5	Nucl. posterior	37 ± 4
Nucl. lateralis pars ventralis	31 ± 7	Pulvinar	39 ± 4
Nucl. arcuatus	45 ± 4	Nucl. geniculatus medialis	44 ± 5
Nucl. dorsomedialis	44 ± 5	Nucl. geniculatus lateralis	52 ± 11
Anterior midline nuclei	45 ± 3	Capsula interna	19 ± 3
Centre median	32 ± 4	Tract. mammillo-thalamicus	20 ± 2
Midline-nuclear group (dorsal portion)	32 ± 3	Tractus opticus	14 ± 1
	Diencephalon (subthalamic centres)		
Tuber cinereum (medial)	30 ± 6	Optic radiation	15 ± 2
Tuber cinereum (lateral)	30 ± 4	Nucl. subthalamicus	37 ± 3
Tuber cinereum (supraoptic)	35 ± 4	Zona incerta	24 ± 1
Nucl. mammillaris medialis		Peduncular zone of nucl. intercalatus (see Fig. 15)	20 ± 3
Cases 1 & 3	56 ± 8		
Case 2	38 ± 5		
	Basal telencephalic centres		
Nucl. caudatus (caput)	38 ± 3	Ansa lenticularis	13 ± 3
Putamen	41 ± 3	Claustrum	25 ± 3
Pallidum externum	31 ± 5	Amygdala (ventral nuclei)	21 ± 2
Pallidum internum	27 ± 5	Amygdala (dorsal nuclei)	29 ± 2
Capula interna	16 ± 3		
	Precentral motor cortex		
Laminae II–IV	39 ± 4	Substantia alba	15 ± 4
Laminae V–VI	33 ± 4		
	Frontal pole		
Laminae II–IV	46·5 ± 3	Substantia alba	16 ± 2
Laminae V–VI	40 ± 7		
	Parietal cortex		
Laminae II–IV	40 ± 4	Substantia alba	16 ± 1
Laminae V–VI	37 ± 5	Insular cortex (general)	34 ± 3
	Occipital cortex		
Laminae II–III	44 ± 6	Laminae V–VI	39 ± 7
Laminae IV	53 ± 10	Substantia alba	16 ± 2

† Anatomical names according to OLSZEWSKI and BAXTER (1954).

TABLE 1 (*cont'd*)

Human brain Distribution of DPN-diaphorase		Human brain Distribution of DPN-diaphorase	
Nucleus†	μg Formazan/0·0434 mm³ tissue	Nucleus†	μg Formazan/0·0434 mm³ tissue
	Temporal cortex		
Laminae II IV	35 ± 3	Substantia alba	16 ± 2
Laminae V–VI	34 ± 3		
	Deep temporal cortex		
Laminae II–IV	37 ± 4	Ammonshorn	42 ± 1
Laminae V–VI	35 ± 2	Fascia dentata	43 ± 5
Substantia alba	15 ± 2		

† Anatomical names according to OLSZEWSKI and BAXTER (1954).

Correlation coefficients for the data in Table 1.

A. Correlation of DPN-diaphorase (man) and succinic dehydrogenase (cat): 0·863.
B. Correlation of DPN-diaphorase (man) and capillarization (cat): 0·932.
C. Correlation of succinic dehydrogenase (cat) and capillarization (cat): 0·879.

of nuclei. Some of the measurements from Table 1 are repeated in Table 2 to facilitate comparison of general gradations and cytological pattern.

A series of photomicrographs (Figs. 1–19) shows the typical patterns of enzyme distribution. Since most of the information concerning them is included in Tables 1 and 2, the following text is limited to certain general conclusions.

A comparison of densitometric and spectrophotometric formazan measurements

The data from the cat brain studies have been included in this paper for comparison of the enzyme patterns in the two species as well as for comparison of the technical reliability of the densitometric and spectrophotometric measurements. The almost identical data obtained by tissue densitometry and by the spectrophotometric measurement of extracted formazan showed that both methods, handled with necessary caution, were reliable and exact for the demonstration of enzyme patterns in the brain. Microscopic densitometry permitted one to focus a small nucleus more closely. The spectrophotometric data provided a general average of the region, sometimes including adjacent tissue with a weaker reaction. Slightly higher densitometric data were marked by an asterisk wherever we felt that the spectrophotometric data included some adjacent tissue with a weaker reaction. The densitometric readings were slightly lower in comparison with the spectrophotometric data in all regions with very weak reaction, particularly in white matter.*

* Data obtained since the submittance of this paper (using both assays and histochemical measurements) indicated that the proportion of gray and white matter was truly greater for succinic dehydrogenase than for DPN-diaphorase.

There has been some recent discussion as to the specificity of various tetrazolium salts. The densitometric data on the cat refer to sections stained with Nitro BT while the spectrophotometric data refer to INT. The nearly identical results do not indicate any significant differences among these tetrazolium salts.

Comparison of cat and human medulla oblongata

An atlas of the distribution of four oxidative enzymes (succinic dehydrogenase, cytochrome oxidase, DPN- and TPN-diaphorase) in the cat brain stem has been published (FRIEDE, 1961*c*). The densitometric measurements of succinic dehydrogenase reported in this atlas are included in Table 1. Comparing the pattern of succinic dehydrogenase in the cat brain with that of DPN-diaphorase in human brain, one was struck by their similarity. The general gradations among nuclei were identical for both species; even detailed gradations within certain nuclei were alike. For example, the portions of the reticular formation which project to the cerebellum (nucl. reticularis paramedianus, nucl. reticularis lateralis, and nucl. reticularis tegmenti of Bechterew) showed markedly stronger enzymic activity than that of the rest of the reticular formation (compare Figs. 2, 3 and 9). Furthermore, the detailed gradations of enzymic activity in the central grey substance were identical in both species: Enzymic activity decreased from the pons to the caudal part of the aqueduct. At the level of the inferior colliculus there was stronger enzymic activity in the dorsal part than in the ventral part of the central gray matter, the latter showing exceptionally weak activity. At the level of the superior colliculus, enzymic activity increased, being strongest in the dorsal-lateral portions. The measurements in the cat cervical cord and cerebellum did not match the human data. This is difficult to interpret without further investigation.

Measurements in the human brain were made only for DPN-diaphorase. Random sections were studied for succinic dehydrogenase and cytochrome oxidase. These enzymes showed the same distribution as DPN-diaphorase. Such observations and the data from the cat brain provide evidence that the patterns of several oxidative enzymes and of capillarization are identical, evidently indicating normal gradations of the oxidative metabolism among nuclei.

Comparison of the diencephalon of man and guinea pig

The enzyme pattern of the medulla oblongata did not seem to change among the species studied. However, in the thalamus there were marked differences between man and guinea pig. The present mapping of DPN-diaphorase and random material on succinic dehydrogenase and cytochrome oxidase in man was compared with the distribution of succinic dehydrogenase (FRIEDE, 1961*a*) and DPN-diaphorase in the guinea pig.

Gradations among thalamic nuclei were much less accentuated in man than in the guinea pig, where the individual nuclei formed quite contrasting patterns. However, considerable gradations of enzymic activity were observed within certain human thalamic nuclei, such as the ventral and lateral nuclei and the pulvinar. These were characterized by irregular bizarre patches of strong enzymic activity. These patterns were too diversified to permit one to distinguish the typical findings from individual variations. Two areas showing distinct species differences, presumably phylogenetic,

TABLE 2. CYTOLOGICAL PATTERNS OF DPN-DIAPHORASE IN THE HUMAN BRAIN

Nucleus*	μg Formazan per 0·0434 mm³ tissue	Distribution Neuropil-Perikarya	Boundaries
		Cervical cord	
Columna ventralis	33 ± 4	Very strong reaction in the large motor neurons and their dendrites; medium reaction in the intervening neuropil (Fig. 1).	Sharp boundaries with white matter.
Columna lateralis	35 ± 5	Very strong reaction in the star-shaped cells, weak reaction in reticular neuropil.	Reticulated processes extend between adjacent tracts.
Tissue surrounding the canalis centralis	24·5 ± 3	Weak to no reaction; very strong reaction in the ependyma, particularly the superficial part of the cells (Fig. 2).	
Dorsal-central groups	30 ± 5	Strong reaction in both cell bodies and intervening neuropil.	Sharp boundaries toward white matter.
Nucl. n. trigemini spinalis:	38 ± 2		
Pars zonalis	Strong	Very strong reaction in the cell bodies and also in the neuropil which has reticular texture.	Sharply delineated reticular cell groups.
Pars gelatinosa	Very strong	Diffusely distributed reaction, no cell bodies distinguishable (Fig. 1).	Less reaction in the peripheral parts of the nucleus.
Pars magnocellularis	Medium	Perikarya show prominent reaction; the irregular, reticular neuropil shows medium activity.	Gradual transition in adjacent nuclei.
		Medulla oblongata	
Ependyma	Strong	Strong reaction in the ependymal cells, underneath the cuticula. Very weak reaction in the subependymal glial tissue.	
Area postrema	Weak	Irregular texture of tissue, some cells contain strong activity.	Gradual transition into nucl. tractus solitarii.
Nucl. gracilis	22·5 ± 3 (caudal) 30 ± 4 (cranial)	Very strong reaction in the cell bodies and the irregular, reticular neuropil, which is arranged in clusters. Conspicuous decrease of the reaction in the cranial portion of the nucleus (Figs. 1, 2).	Nucleus sharply defined from tracts; the shape of the nucl. is very irregular.
Nucl. cuneatus lateralis	44 ± 5	Very strong reaction in cells and neuropil; the latter is extremely irregular and forms compact clusters. (Fig. 3).	Sharply defined toward white matter; some cells scattered outside of the neuropil.

* Anatomical names according to OLSZEWSKI and BAXTER (1954).

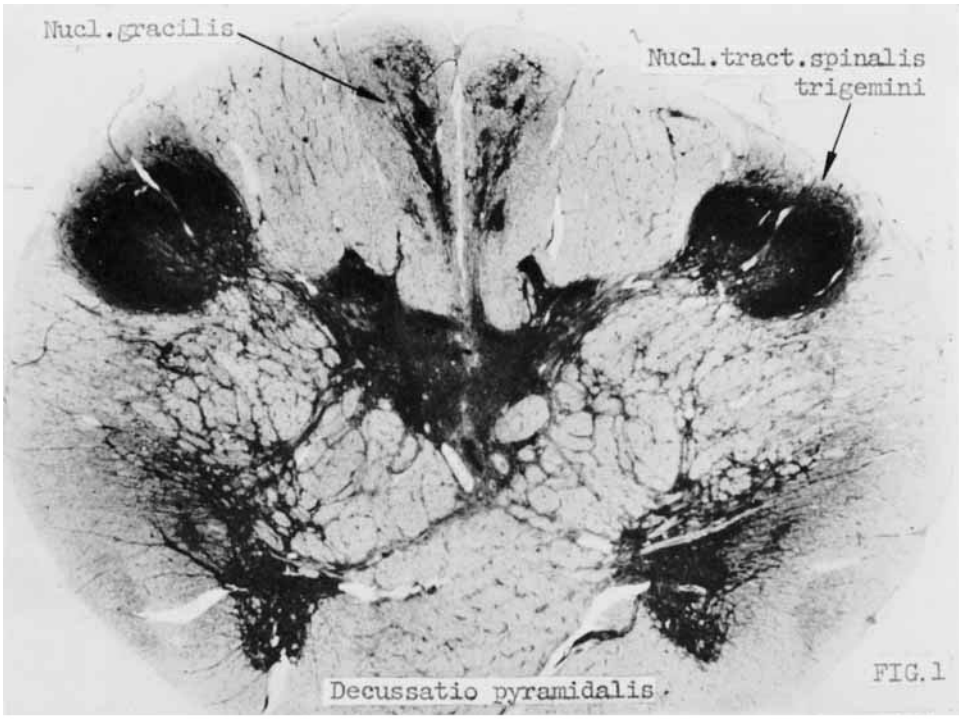

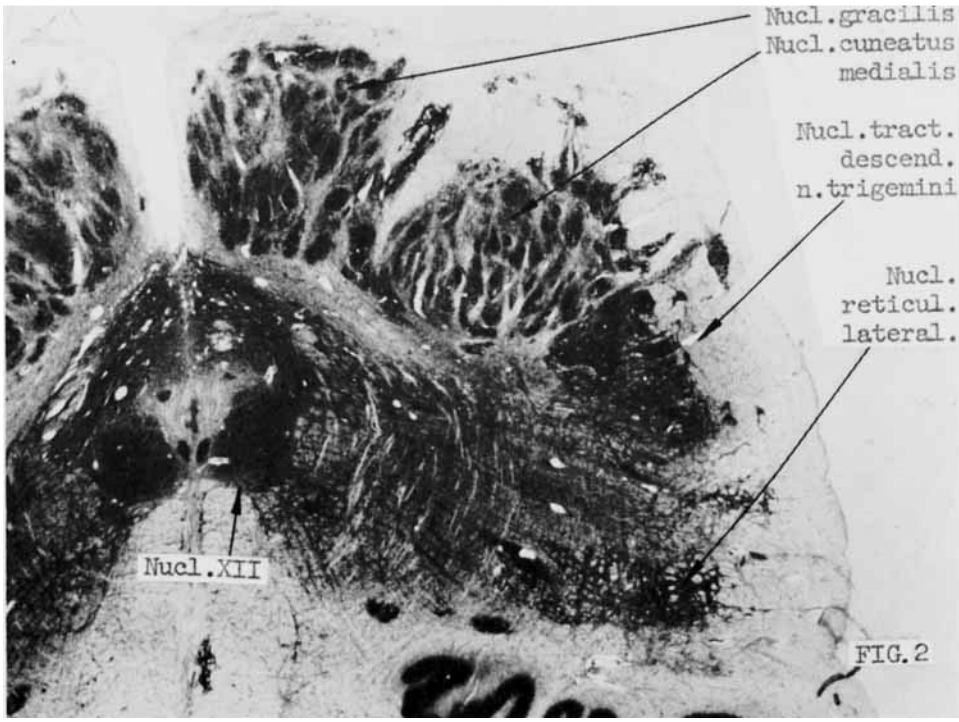

FIG. 1.– Cervical cord approximately at the level of C.1.
FIG. 2.—Medulla oblongata caudal to the fourth ventricle (the ventral portion of the section was deleted because of its identity with Fig. 3).
Consult Table 2 for a detailed description of the nuclei labelled. Both figures demonstrate DPN-diaphorase activity in 30 μ sections.

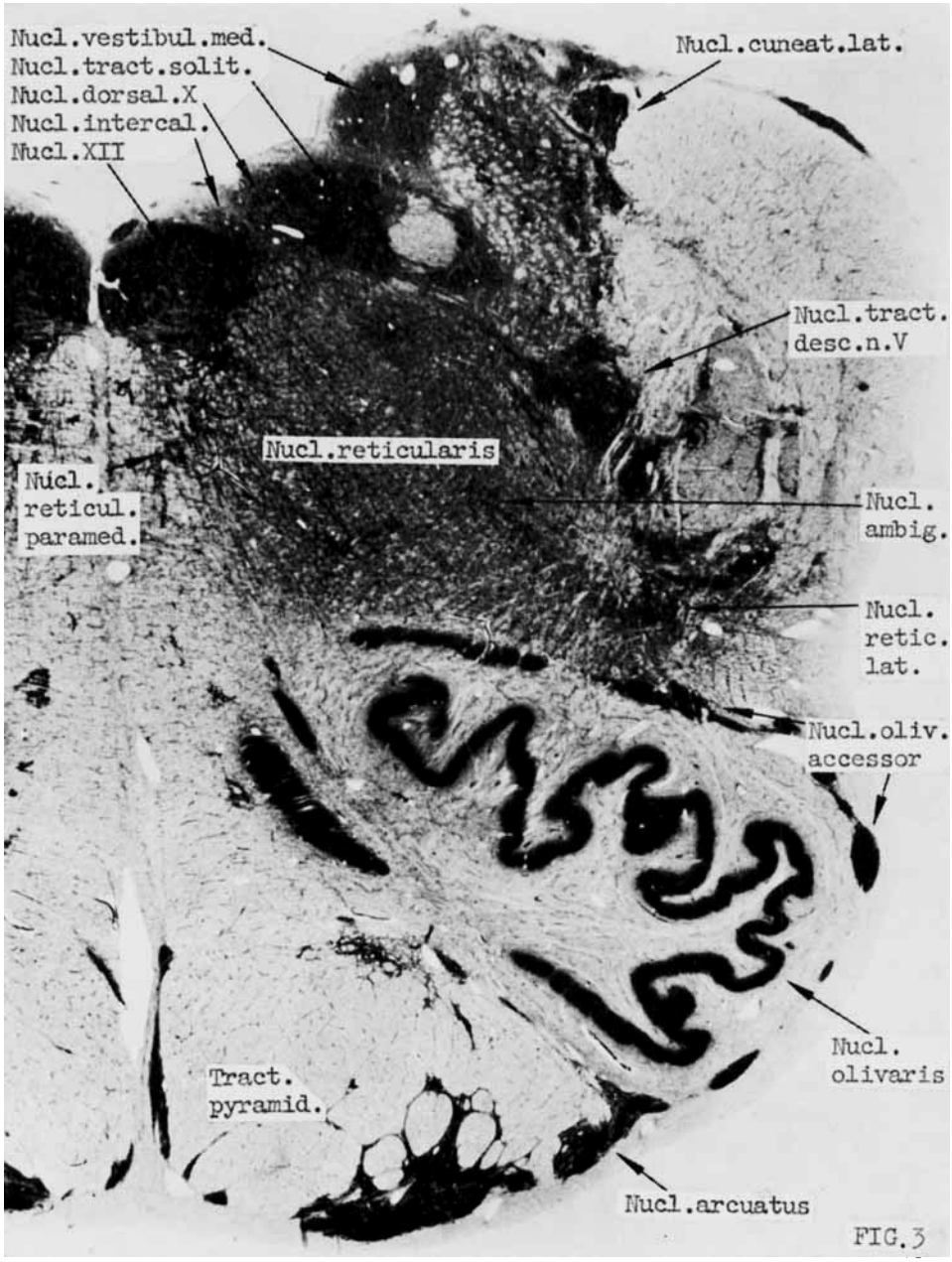

FIG. 3.—Medulla oblongata level of the hypoglossal nucleus. Consult Table 2 for a detailed description of the nuclei labelled. The figure demonstrates DPN-diaphorase activity in 30 μ sections

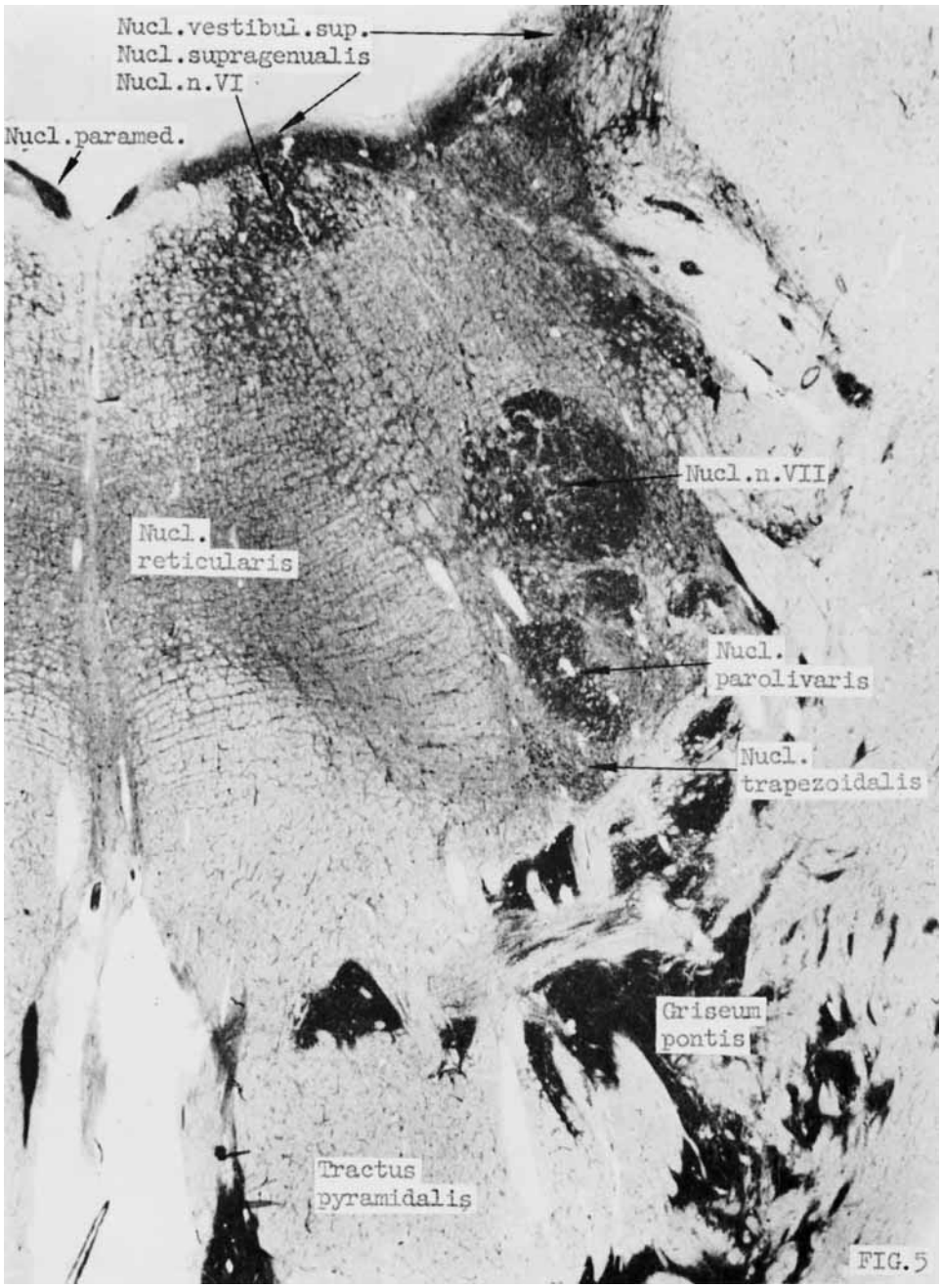

FIG. 4.—Medulla oblongata; level of the vestibular nuclei. Consult Table 2 for a detailed description of the nuclei labelled. The figure demonstrates DPN-diaphorase activity in 30 μ section.

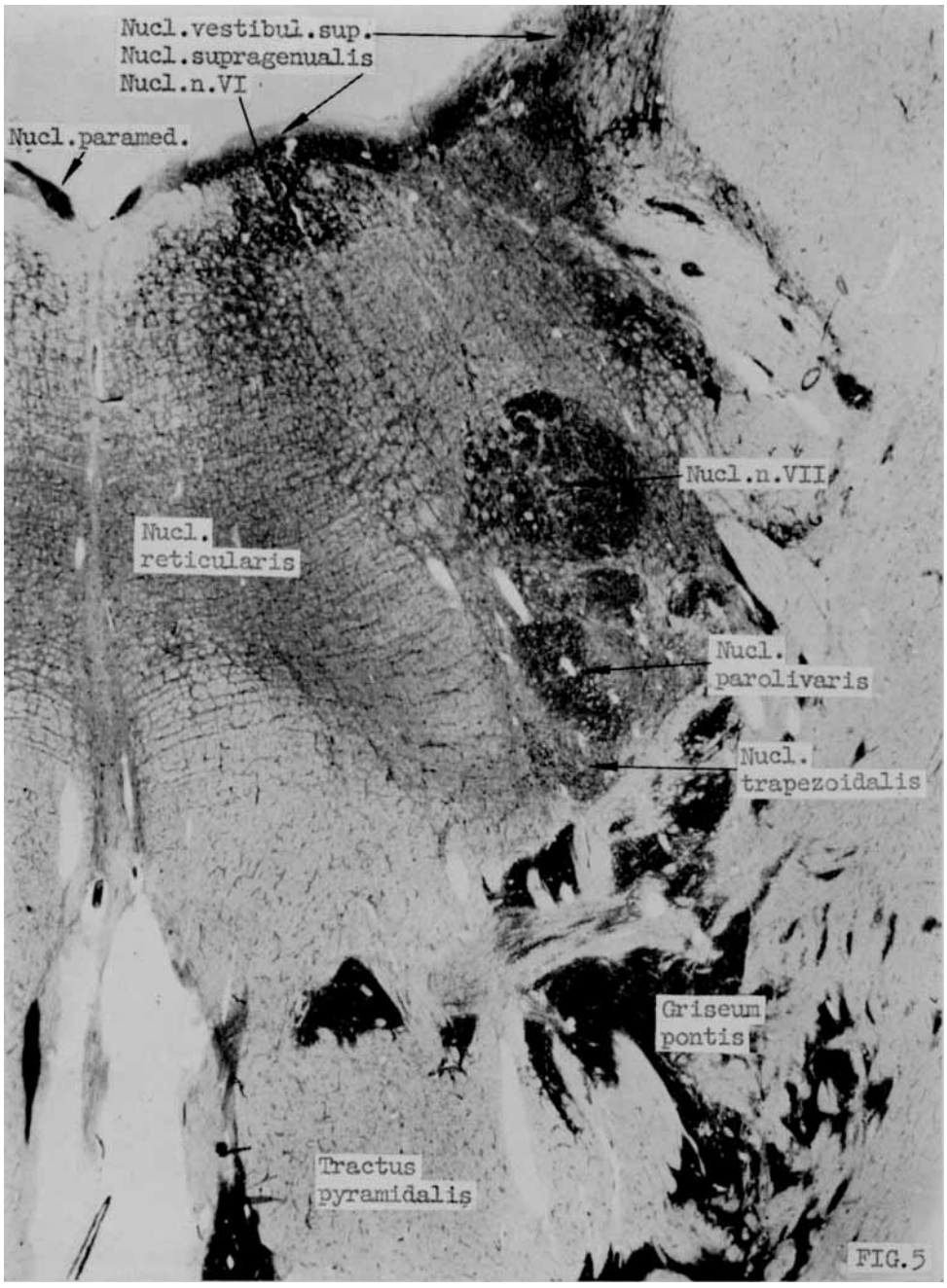

FIG. 5. Pons, caudal portion. Consult Table 2 for a detailed description of the nuclei labelled. The figure demonstrates DPN-diaphorase activity in 30 μ section.

TABLE 2. (*cont'd*)

		Medulla oblongata—(*cont'd*)	
Nucl. n. hypoglossi	43 ± 5	Very strong reaction in the motor cells; dendrites are distinguishable in the reticular neuropil (Fig. 3).	Boundaries well defined by the strong reaction in the neuropil.
Nucl. Roller	Strong	Enzyme pattern similar to XII, but distinguished by stronger reaction in the neuropil.	Borders defined by strong reaction in the neuropil.
Nucl. intercalatus	Medium	Diffusely distributed weak reaction with some nerve cells distinguishable (Fig. 3).	Sharply delineated area of neuropil.
Nucl. dorsalis vagi	28 ± 4	Strong reaction in neurons and their dendrites, in contrast to the weak reaction in intervening neuropil. Pigmented cells have little activity (Fig. 3).	Neuropil blends with the nucl. tract. solitarii.
Nucl. tractus solitarii	28 ± 4	Diffusely distributed weak reaction throughout the neuropil, no cells are distinguishable, except in the magnocellular part, where a strong reaction is found in nerve cells (Fig 3).	Blending of neuropil with nucl. dors. vagi and A. postrema.
Nucl. tractus descendentis n. trigemini	39 ± 5	Diffuse reaction in the somewhat irregular neuropil with almost no cells distinguishable. The cranial extensions of the pars gelatinosa of the spinal nucleus are well distinguished by their homogeneous neuropil (Figs. 2-5).	Sharp borders laterally; transition into formatio reticularis medially.
Nucl. reticularis:	30 ± 5		
Pars medialis	Medium	Very strong reaction in the large cells and their long dendrites; weak reaction in the reticular neuropil (Fig. 4).	Diffuse transition or blending with adjacent nuclei.
Pars lateralis	Medium	Fewer cells distinguished than in the medial part; diffusely distributed reaction in the neuropil.	
Nucl. reticularis paramedianus	Strong	This nucleus is distinguished by a stronger reaction in the neuropil and probably also in the cell bodies (Fig. 3).	Reticular bridges of neuropil to the nucl. reticularis; these are outlined by a strong reaction.
Nucl. reticularis gigantocellularis	Strong in cells	Very strong reaction in the cells and their dendrites; weak reaction in the neuropil (Fig. 5).	Distinguishable by the distribution of cells with strong reaction.
Nucl. subtrigeminalis (Nucl. reticularis lateralis)	Strong	Strong reaction in the dense neuropil. Resembles closely the nucl. reticularis paramedianus (Figs. 2, 3).	Strong reaction in the neuropil.
Nucl. ambiguus	Strong in cells	Nerve cells and their dendrites show a contrasting strong reaction; weak reaction in the neuropil (Fig. 3).	Neuropil blends with the surrounding formatio reticularis.

TABLE 2 (*cont'd*)

Nucleus*	μg Formazan per 0·0434 mm^3 tissue	Distribution Neuropil-Perikarya	Boundaries
		Medulla oblongata—(*cont'd*)	
Nucl. olivaris and nucl. parolivaris	57 ± 9·5	Very strong reaction in the cell bodies which are clearly distinguishable; strong and homogeneously distributed reaction in the intervening neuropil.	Very sharp borders; most of the cells are within the neuropil, some are scattered outside of it.
Nucl. arcuatus		Very strong reaction in the cells, strong and diffusely distributed reaction in the neuropil. (This nucleus resembles the griseum pontis) (Fig. 3).	Very sharp boundaries.
Nucl. paramedianus dorsalis caudalis and dorsalis oralis		Neuropil with a homogeneously distributed strong reaction. Some cells show a very strong reaction. (Fig. 5).	Very sharp.
Nucl. prepositus hypoglossi	37 ± 8	Weak to medium reaction in the neuropil; only some of the cells are demonstrated by a strong reaction (Fig. 4).	Neuropil blends with nucl. hypoglossi and nucl. vestibularis medialis.
Nucl. cochlearis	Strong in cells	Strong reaction in the cells and their short dendrites; the neuropil is scanty and 'flocculated' (Fig. 4).	Sharp borders.
Tuberculum acousticum	47 ± 6	The upper layer shows a diffuse reaction in the neuropil, and no cells are visible. The deep layer shows a strong reaction in cells and scanty reaction in the neuropil.	Sharp borders.
Nucl. vestibularis medialis	43 ± 4	Diffuse reaction in the neuropil; only a fraction of the cell population is discernible by a strong reaction (Fig. 4).	Transition into the nucl. prepositus hypoglossi. Sharp borders with the nucl. vestibularis lateralis.
Nucl. vestibularis caudalis	Medium	The reticular neuropil is scattered between the descending fibre tracts; few nerve cells are distinguishable.	This nucleus shows transition into most of the adjacent nuclei.
Nucl. vestibularis lateralis (Deiters)	33 ± 4	Very strong reaction in Deiters cells and in their long dendrites. There is little and scanty neuropil with a weak reaction (Fig. 4).	
N. vestibularis superior (Bechterew)	26 ± 3	Neuropil with medium reaction and an irregular 'patchy' structure; only a few cells are distinguished by strong reaction (Fig. 5).	Transitions into the lateral vestibular nucleus and the central gray.

* Anatomical names according to OLSZEWSKI and BAXTER (1954).

TABLE 2 (*cont'd*)

		Cerebellum	
Nucl. fastigii, globosus and emboliformis	46 ± 1	Strong reaction in the cells, extending far into the dendrites; the latter are clearly demonstrated, since there is very little neuropil (Fig. 7).	Sharply defined by the surrounding white matter.
Nucl. dentatus	55 ± 8·5	Very strong reaction in cells, strong reaction in the neuropil in which many dendrites are discernible. Many cells are situated outside of the neuropil while their dendrites project into the neuropil (Fig. 7).	Very sharp borders.
Cerebellar cortex:			
Stratum moleculare	33 ± 5	Diffusely distributed reaction, high power shows a delicate network of dendrites. Large dendrites of Purkinje cells are outlined by strong reaction (Fig. 6).	
Purkinje cells	Strong	Very strong reaction in the perikarya, weak reaction in the intervening glial tissue (Fig. 6).	
Stratum granulare	32 ± 7	Excessively strong reaction in the synaptic glomerula cerebellaria. Almost no reaction in the perikarya of the granular cells (Fig. 6).	
		Pons	
Nucl. n. trigemini motorius	39 ± 9	Very strong reaction in the motor cells; strong reaction in the neuropil which has a reticular texture.	The neuropil is well delinated.
Nucl. n. trigemini sensibilis principalis	31 ± 11	Compact, homogeneous neuropil with a strong reaction; the neuropil is arranged in irregular clusters. Nerve cells are not discernible.	The nucleus appears as an aggregation of clusters of neuropil which are individually well defined.
Nucl. abducentis	34 ± 5	Resembles the motor trigeminal nucl. (Fig. 5).	Sharp borders.
Nucl. n. facialis	Strong	Very strong reaction in the motor cells, strong reaction in the homogeneous neuropil which is perforated by fibre bundles. (Fig. 5).	Very sharp borders with the nucl. olivaris superior. Transitions of neuropil with nucl. reticularis.
Nucl. olivaris superior principalis	≈42 ± 7	Very strong reaction in the medium-sized nerve cells; their dendrites blend with a dense, reticular neuropil with strong reaction.	Sharp borders

TABLE 2 (*cont'd*)

Nucleus*	μg Formazan per 0·0434 mm³ tissue	Distribution Neuropil-Perikarya	Boundaries
		Pons—(*cont'd*)	
Nucl. olivaris superior lateralis (nucl. parolivaris)	≈42 ± 7	Unique pattern of very strong reaction in the fusiform cells and their long dendrites which run approximately parallel to each other. Almost no reaction in the neuropil. The reaction in cells resembles the pallidum, but the arrangement of the cells and their dendrites is specific for this nucleus (Fig. 5).	Dendrites can be traced into the adjacent tissue.
Nucl. trapezoidales	Strong in cells	Round cells with a strong reaction; scarce neuropil; the dendrites are poorly demonstrated. (Fig. 5).	Borders not sharp.
Nucl. reticularis pontis	25 ± 4	Same enzyme distribution as in the medulla oblongata. (Pars medialis and lateralis) (Fig. 9).	
Nucl. papilioformis (nucl. reticularis Bechterew	48 ± 5	Very strong reaction in the cell bodies; the neuropil has a distinctly stronger reaction than the adjacent nucl. reticularis. Many dendrites are distinguishable in the neuropil which has a reticular texture similar to the nucl. reticularis paramedianus. The neuropil of the griseum pontis is more compact and has a stronger reaction.	The neuropil is sharply delineated from the rest of the reticular formation by its stronger reaction.
Griseum pontis	47 ± 3	Strong reaction in both the cells and the dense, homogeneous neuropil. There is variation among regions of the griseum pontis (Fig. 8).	Very sharp delineation of the neuropil.
Nucl. parabrachialis	22 ± 3	Diffuse reaction in the neuropil, which has a "patchy" structure. No cells are distinguishable (Fig. 9).	The neuropil extends between the fibre bundles of the brachium conjuctivum.
Griseum centrale (pons)	23 ± 7	Diffuse weak reaction in the neuropil; no cells distinguishable (Figs. 9, 10).	Transitions into many adjacent nuclei.
Nucl. supratrochlearis (nucl. centralis sup. dors.)	Strong in cells	Strong reaction in the cells; medium reaction distributed diffusely in the neuropil (Fig. 10).	Borders defined only by the distribution of the cells.

* Anatomical names according to OLSZEWSKI and BAXTER (1954).

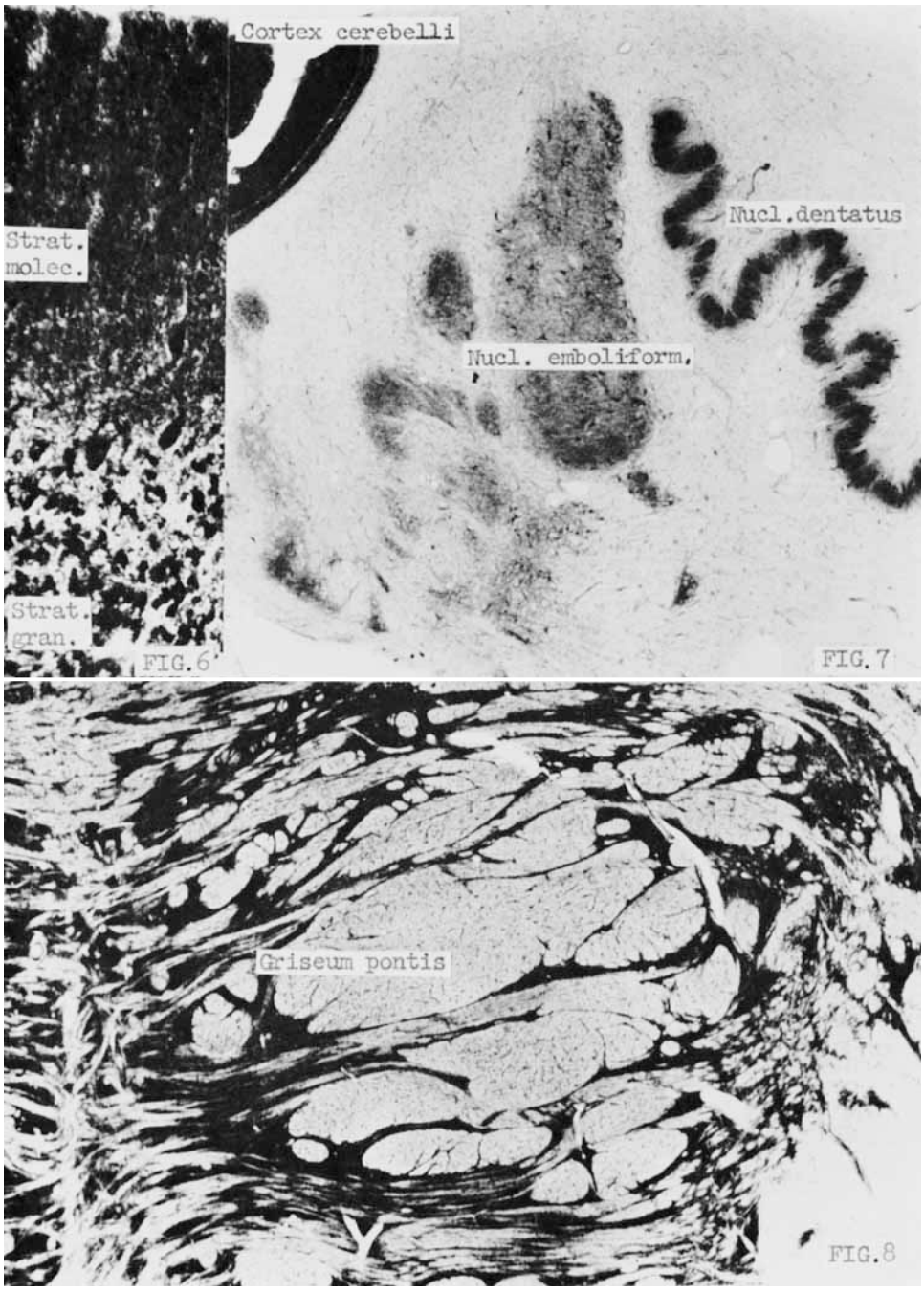

FIG. 6. High power enlargement of the cerebellar cortex (compare Fig. 7 for reference).
FIG. 7.—Cerebellar nuclei.
FIG. 8.—Pontine grey.
Consult Table 2 for a detailed description of the nuclei labelled. All figures demonstrate DPN-diaphorase activity in 30 μ sections.

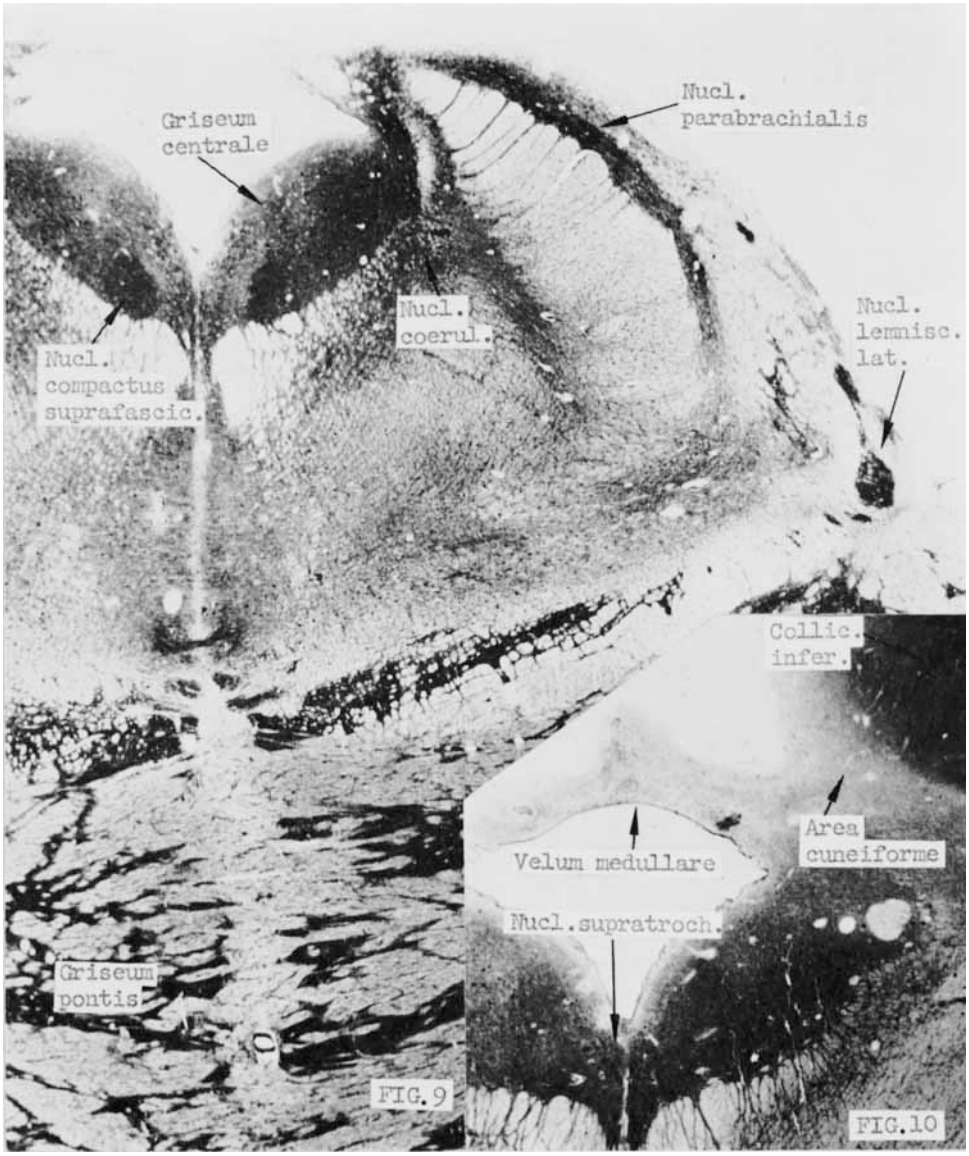

FIG. 9.—Pons; level of the oral portion of the fourth ventricle.
FIG. 10.—Velum medullare anterius; level of the caudal orifice of the aqueduct.
Consult Table 2 for a detailed description of the nuclei labelled. Both figures demonstrate DPN-diaphorase activity in 30 μ sections.

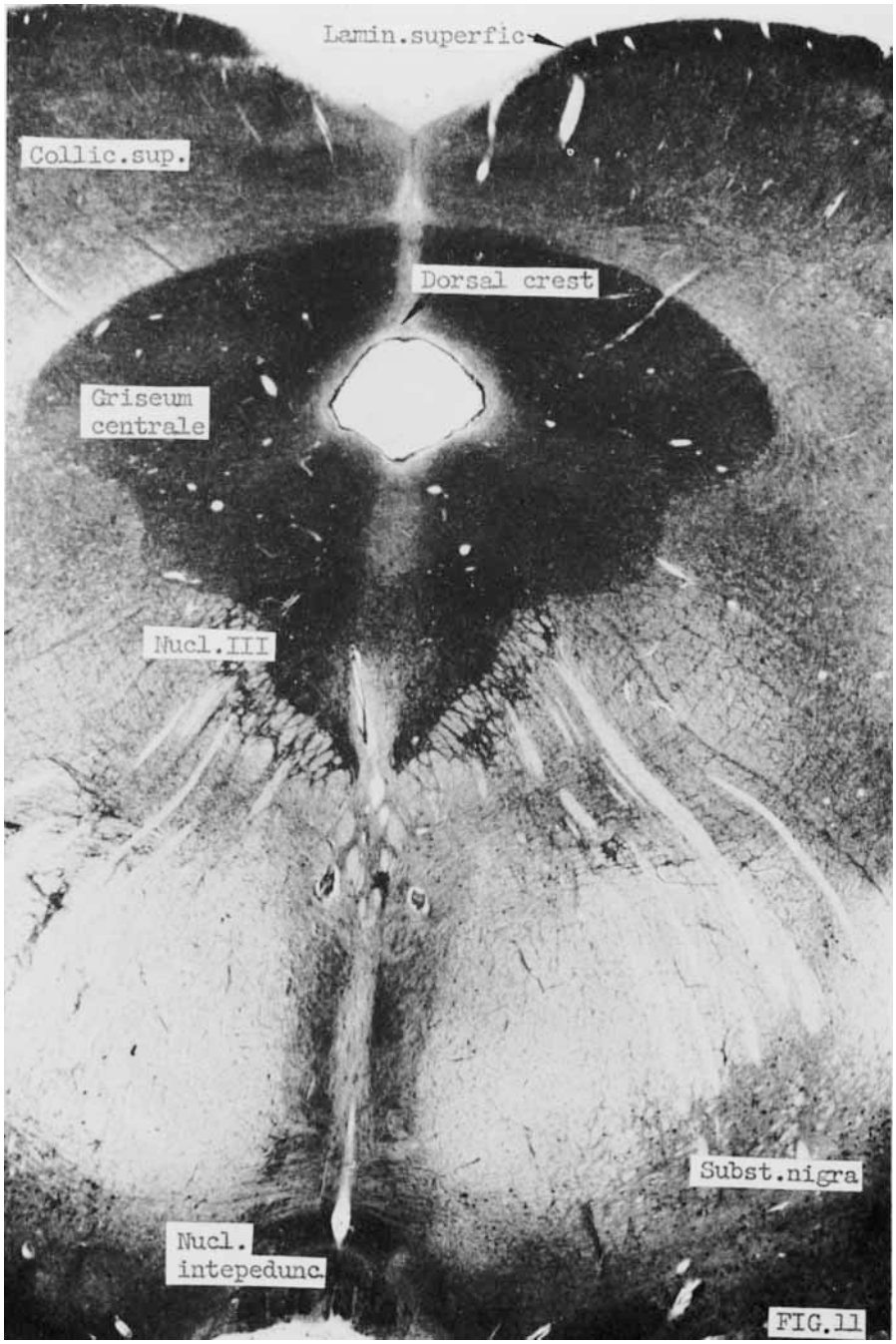

FIG. 11.— Midbrain; level of the upper colliculi. Consult Table 2 for a detailed description of the nuclei labelled. The figure demonstrates DPN-diaphorase activity in 30 μ section.

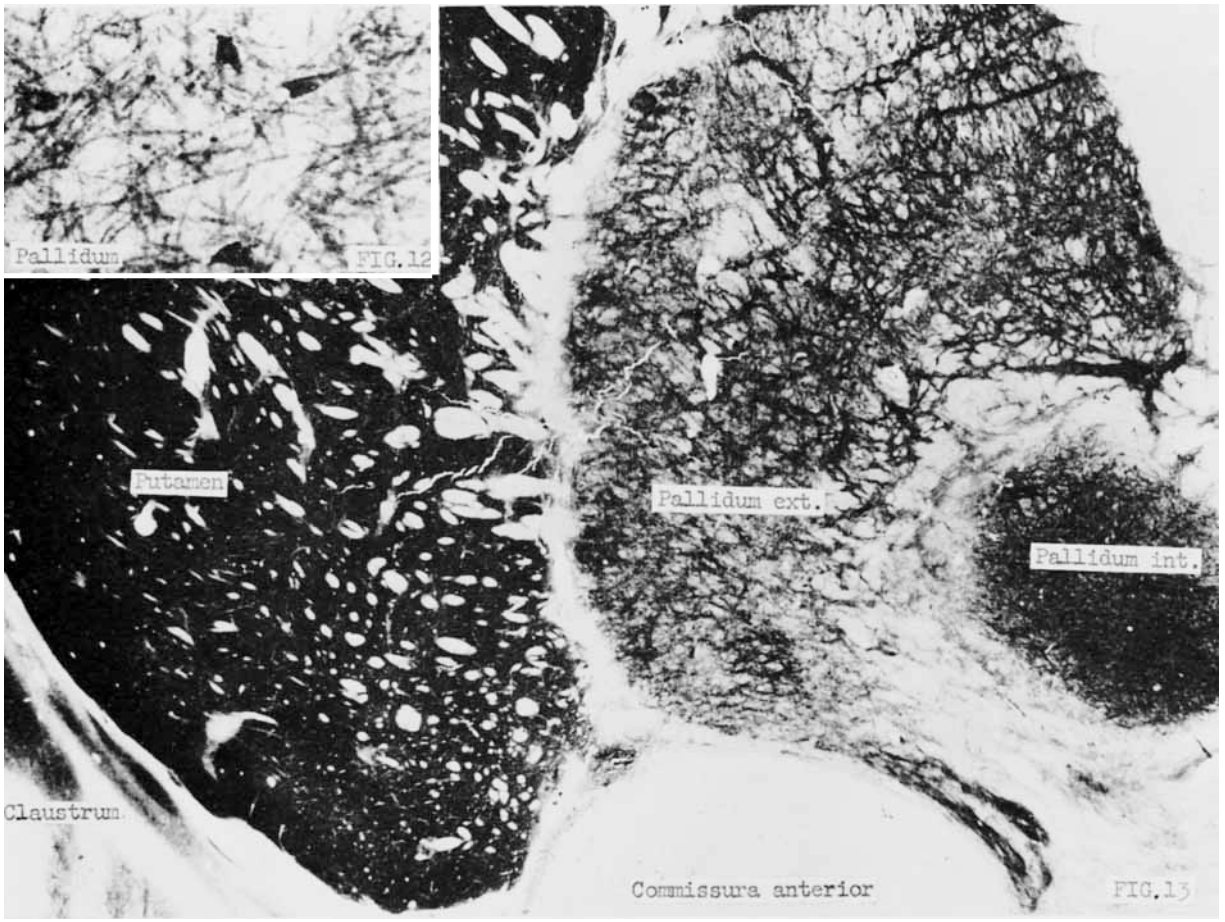

FIG. 12.—Putamen and pallidum.
FIG. 13.—High power enlargement of the pallidum.
Consult Table 2 for a detailed description of the nuclei labelled. The figures demonstrate DPN-diaphorase activity in 30 μ sections.

TABLE 2 (*cont'd*)

		Pons—(*cont'd*)	
Nucl. coeruleus	19 ± 1	Diffuse reaction in the neuropil; medium reaction in the nerve cells. Succinic dehydrogenase appears to be weak in nerve cells (Fig. 9).	No distinct borders of the neuropil.
Nucl. compactus suprafascicularis	Strong	Strong reaction distributed diffusely in the neuropil; cells are not distinguishable (Fig. 9).	The neuropil has sharp borders indicated by a sudden decrease of activity.
		Mesencephalon	
Marginal glial layer		No or extremely weak enzyme activity.	Sharp boundaries with the neuropil.
Posterior colliculus	51 ± 3 (caudal) 37 ± 3 (cranial)	Strong diffusely distributed reaction in the neuropil from which no cells are distinguishable (Fig. 10).	Sharp boundaries of the neuropil.
Griseum centrale (level of the aqueduct)	32 ± 3 (dorsal) 17 ± 2 (ventral)	Homogenous distribution of a weak reaction in the neuropil; few cells are discernible. The dorso-rostal portion of the griseum centrale has a stronger reaction than the ventro-caudal portion (Fig. 11).	No sharp boundaries; transitions in many adjacent nuclei.
Area cuneiforme	23 ± 2	Weak reaction in the scanty neuropil; there is strong reaction in some of the large nerve cells (Fig. 10).	Poorly defined borders.
Nucl. dorsalis raphes	Weak	Very weak reaction; no cellular details distinguishable.	Sharply separated from the neuropil of the adjacent central gray.
Nucl. parabrachialis	25 ± 4	Weak reaction in both nerve cells and the neuropil (reaction is weaker than that in the substantia nigra).	Fairly sharp delineation by adjacent fibre bundles.
Nucl. lemnisci lateralis	Medium	Strong reaction in neurons, medium in the neuropil (Fig. 9).	Sharp boundaries.
Nucl. ruber	25 ± 3 (magnocell.) 31 ± 3 (transition) 42 ± 7 (parvocell.)	Strong reaction in the large cells and their dendrites; little reaction in the neuropil. The small cells are less distinct.	Sharp boundaries.
Substantia nigra	26 ± 2	Complex chemical architecture exhibiting considerable local variations of pattern: *Pars reticularis:* medium reaction in the cells and their dendrites; the neuropil appears as a network of long dendrites. *Pars compacta:* Weak reaction in the neuropil; the reaction in cells varies; most cells have little activity and there is an inverse relationship of pigmentation and enzyme activity. Very long dendrites extend between the fibre bundles of the adjacent cerebral peduncles (Fig. 11).	Neuropil tends to blend with adjacent nuclei; the boundaries are quite indistinct.

TABLE 2 (*cont'd*)

Nucleus*	µg Formazan per 0·0434 mm³ tissue	Distribution Neuropil-Perikarya	Boundaries
		Mesencephalon—(*cont'd*)	
Nucl. paranigralis	Strong	Stronger reaction than in the nucl. interpeduncularis. The neuropil has a reticular 'dendritic' pattern; some cells are visible.	Sharply delineated from the nucl. interpeduncularis.
Nucl. interpeduncularis	Medium	Medium reaction somewhat irregularly distributed in the neuropil. No cells distinguishable (Fig. 11).	Sharp boundaries.
Superior colliculus	43 ± 3 (lamina superfic.) 35 ± 4 (lamina profound.)	Very strong reaction in the molecular layer; medium reaction in the deeper cellular layers; weak reaction in the fibre laminae. In all these regions, the reaction is found in the neuropil; very few cells are distinguishable. Large nerve cells with a strong reaction are seen in the lateral ventral portion of the deeper layers (Fig. 11).	Sharply delineated toward the griseum centrale. Blending of the neuropil with the reticular formation.
Nucl. n. oculomotorii	51 ± 2	Very strong reaction in the cells and dendrites, strong reaction in the neuropil which has a reticular texture (Fig. 11).	Borders are defined by stronger reaction in the neuropil.
Nucl. of Edinger-Westphal	Weak	Reaction in nerve cells; very weak reaction in the neuropil.	Sharply separated from the adjacent neuropil of the central gray.
Nucl. Darkschewitsch	Medium	Spotted neuropil defined by stronger reaction than in the adjacent griseum centrale. Scattered nerve cells with very strong activity are observed.	Indistinct boundaries.
Nucl. interstitialis (Cajal)	Reaction in cells	Strong reaction in cells; there is little reticular neuropil which resembles that of the nucl. ruber.	Well distinguished from the nucl. Darkschewitsch by the texture of the neuropil.
		Thalamus (only the more important nuclei are listed)	
Nucl. anterior dorsalis	Strong 45 ± 4	Very homogeneous distribution of a strong reaction in the neuropil; scattered large nerve cells are clearly distinguishable (Fig. 15).	Sharp boundaries.
Nucl. anterior lateralis	Strong	Contrary to the nucl. ant. dors., the reaction in the neuropil is very unhomogeneous or 'flocculated'; many perforating fibre bundles are present; large cells are distinguishable by strong reaction.	Sharp boundaries of the neuropil.

* Anatomical names according to OLSZEWSKI and BAXTER (1954).

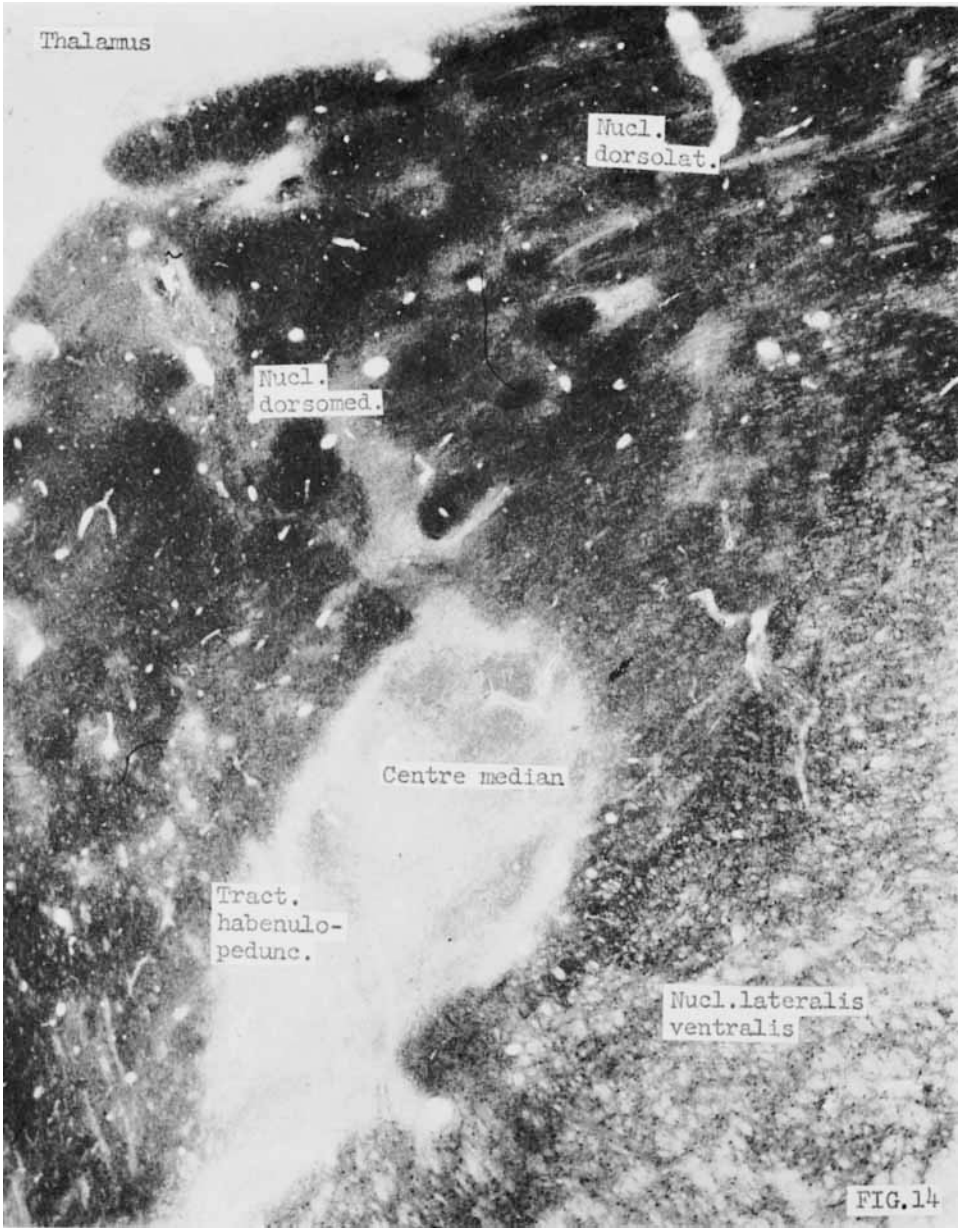

FIG. 14.—Thalamus, middle portion. Consult Table 2 for a detailed description of the nuclei labelled. The figure demonstrates DPN-diaphorase activity in 30 μ section.

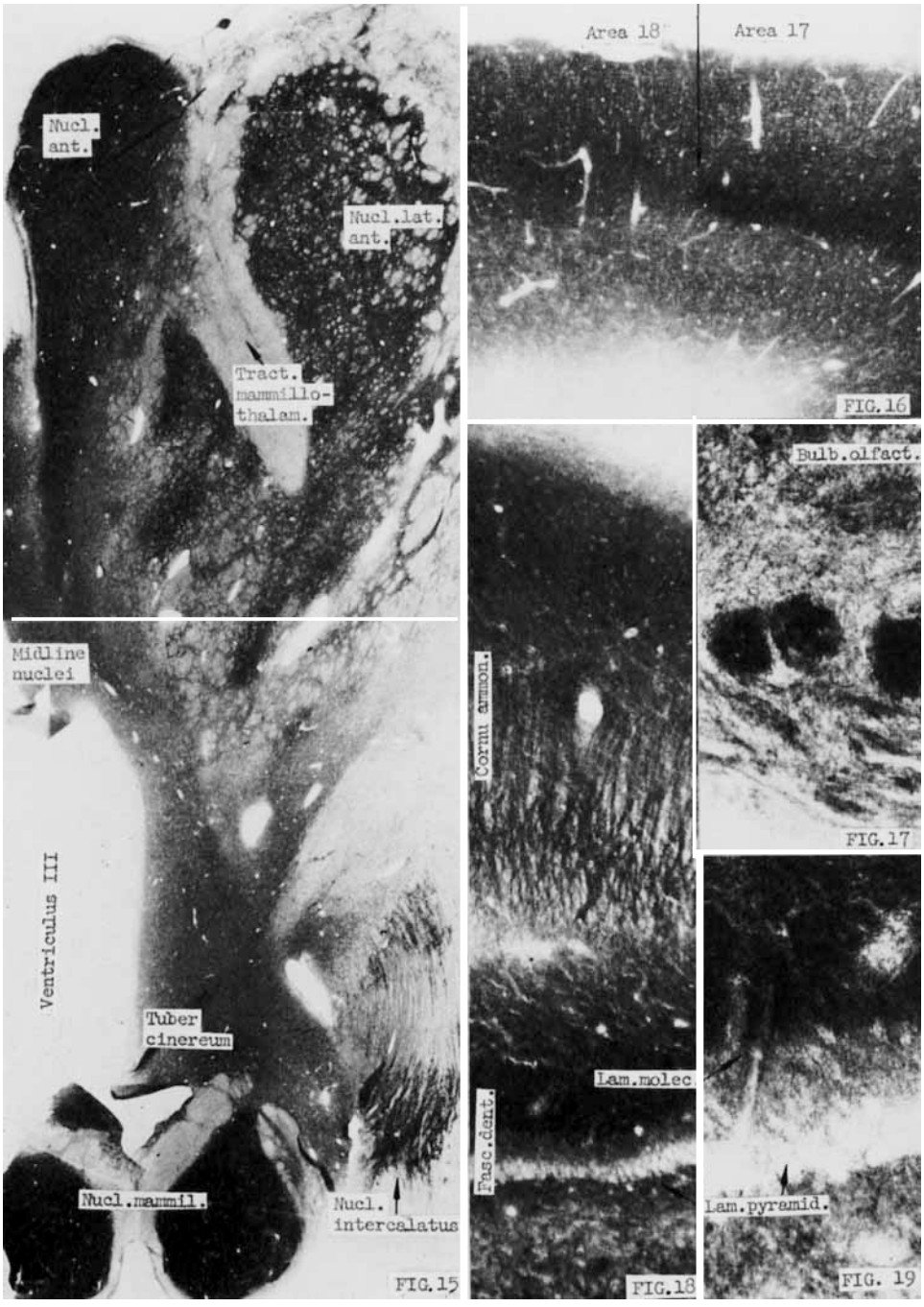

FIG. 15. –Thalamus and hypothalamus, anterior portion.
FIG. 16.—Cerebral cortex; border between area 17 and 18.
FIG. 17.—High power enlargement of the olfactory bulb.
FIG. 18. –Survey of the layers of the cornu ammonis and the fascia dentata.
FIG. 19.- High power enlargement of the fascia dentata.
Consult Table 2 for a detailed description of the nuclei labelled. All figures demonstrate DPN-diaphorase activity in 30 μ sections.

TABLE 2 (*cont'd*)

		Thalamus—(*cont'd*)	
Nucl. dorsomedialis	44 ± 5	Very inhomogeneous reaction in the neuropil, patchy pattern, frequently perforated by fibre bundles. Local variations of intensity. Medium sized cells with a very variable reaction are distinguishable (Fig. 14).	
Nucl. lateralis	Medium 42 ± 5 (dorsal) 31 ± 7 (ventral)	Gradual change in pattern from dorsal to ventral. Dorsal: diffuse reaction in the neuropil, there are no cells distinguishable. Toward ventral there is a gradual increase of the reaction in the cells. In the most caudal portion these cells resemble those of the nucl. reticularis. Many perforating fibre bundles are seen (Fig. 14).	The nucleus, as a complex, is sharply delineated; within the nucleus there are no sharp subdivisions.
Centre median	32 ± 4	Very weak, diffusely distributed reaction. No cells are distinguishable (Fig. 14).	The nucleus appears as a conspicuous, sharply delineated light area among the thalamic nuclei.
Pulvinar	39 ± 4	Very irregular pattern: A diffuse reaction is found in the neuropil, but it shows considerable local changes. The reaction in cells varies; it is prominent in the dorsal portion. Occipitally, there is a more homogeneous enzyme pattern.	Sharp boundaries.
Nucl. reticularis thalami	Reaction in cells	Strong reaction in cells and dendrites; there is a scanty 'flocculated' neuropil.	The nucleus is defined by the distribution of its characteristic cells rather than the neuropil.
Nucl. geniculatus lateralis	52 ± 11	Very strong reaction in the cells, strong reaction in the homogeneously distributed neuropil.	The neuropil of the individual laminae is sharply delineated.
		Hypothalamus	
Hypothalamic gray	30 ± 4	Very homogeneous distribution of a weak reaction in the neuropil. Cells are not distinguishable in the medial portion; the lateral portion shows cells with a strong reaction in a very irregular distribution. Individual nuclei are not delineated from each other except the supraoptic and paraventricular nucleus which are barely distinguished by weak activity in their cells (Fig. 15).	No sharp boundaries, there is a diffuse transition of the neuropil into the thalamic midline nuclei and other adjacent nuclei.

TABLE 2 (*cont'd*)

Nucleus*	μg Formazan per 0·0434 mm³ tissue	Distribution Neuropil-Perikarya	Boundaries
		Hypothalamus—(*cont'd*)	
Nucl. mammillaris	≈56 ± 8	*Medial nucleus:* strong reaction diffusely distributed in the neuropil (Fig. 15). Very strong reaction in the cells, some of which are found outside of the neuropil. *Lateral nucleus:* Very strong reaction, prevailing in the nerve cells.	Very sharp boundaries.
Corpus subthalamicum	37 ± 3	Medium reaction distributed diffusely in the neuropil; cells with short axonal hillock exhibit a strong reaction.	Very sharp delineation of the homogeneous distribution of the reaction in the corpus subthal. and the reticular distribution in the substantia nigra.
		Basal telencephalic centres	
Putamen Nucl. caudatus	41 ± 3 38 ± 3	The putamen shows a very homogeneously distributed, strong reaction in the neuropil. Large nerve cells occasionally are distinguishable by a stronger reaction. The neuropil is sharply delineated from the adjacent white matter, as well as from the perforating fibre bundles and the central gray (Fig. 13).	
Pallidum	31 ± 5 (ext.) 27 ± 5 (int.)	Generally, the reaction is much weaker than that in the putamen; however, there is a strong reaction at the membranes of the nerve cells and dendrites. Dendrites are seen over long distances. The neuropil is scarce. The internal and external portion of the pallidum show similar patterns. Long dendrites may deviate between the fibre bundles of adjacent tracts (Figs. 12, 13).	
Claustrum	25 ± 3	Diffusely distributed neuropil with a weak reaction. Cells are distinguishable (better in the ventral part) however, they show only weak or medium reaction. Many cells are scattered outside of the neuropil (Fig. 13).	

* Anatomical names according to OLSZEWSKI and BAXTER (1954).

TABLE 2 (*cont'd*)

		Basal telencephalic centres—(*cont'd*)
Amygdala	21 ± 2 (vent.) 29 ± 2 (dorsal)	The nuclei of the amygdala form a complex of diffusely distributed weak reaction in the neuropil. The neuropil of the individual nuclei is sharply delineated in the dorsal portion; ventrally, there is transition into the adjacent pyriforme cortex. A fraction of the cell population can be distinguished from the neuropil by slightly stronger reaction. The nuclei are graded as follows: posterior ventralis, posterior internus; superior ventralis; posterior lateralis; posterior medialis, superior amygdalae, and basalis, the latter showing weakest reaction.
Cerebral cortex		Description in the text.

were the centre median and the dorso-medial nucleus. As the histochemical sections clearly demonstrated (Fig. 14), the human brain showed a well defined centre median with low enzyme activity appearing as a 'punched out' area; this pattern was not observed in the guinea pig. The human dorso-medial nucleus had relatively strong enzyme activity in contrast to the weak activity of the homologous region in the guinea pig. This was in accordance with the findings for the fronto-polar cortex which likewise had strong activity in man and weak activity in the guinea pig. The extra thalamic diencephalic centres had similar enzyme patterns in both species, such as the weak activity in the hypothalamus, or the contrasting differentiation of the corpus subthalamicum (strong reaction) from the substantia nigra (weak reaction).

These observations indicate a tendency of caudo-cranial differentiation of the chemo-architecture of the brain. The human thalamus resembled only general outlines of the guinea pig pattern, while the patterns in the medulla oblongata were alike.

Cerebral isocortex. The enzyme patterns in the areas of human isocortex were similar to each other in principle but showed minor variations in the individual areas. The upper four layers showed diffusely distributed enzyme activity in the neuropil, in which only a few perikarya of pyramidal cells were distinguishable by stronger enzymic activity. There was an increase of enzyme activity from the first, or molecular, layer toward the second and third layers. The fifth and sixth layers showed a decrease of enzyme activity in the neuropil; many, but not all of the pyramidal cells exhibited strong activity in their perikarya and the proximal dendrites; there were considerable gradations of activity among individual pyramidal cells. This general pattern varied among the cortical areas as to the thickness of the layers, the number of perikarya with strong enzymic activity and a finer gradient of activity in the neuropil. However, the present large cortical material revealed such an abundance of minor differences among specimens and regions that it was difficult to distinguish the typical features of an area from individual variations. The visual cortex (Area 17) and the postcentral region were characterized by a thin lamina of very strong enzyme activity in the fourth layer; this lamina terminated sharply at the borders of the optic area (Fig. 16), while it showed smoother transitions in the postcentral region. Spectrophotometric measurements of formazan revealed the typical gradations among regions as found in the guinea pig cortex (FRIEDE, 1960); however, the differences among areas were less accentuated in man than in the guinea pig. For both species, gradations among cortical areas were characteristic in the IInd to IVth layers; the temporal cortex showed weakest enzyme activity, having less than the frontal and the parietal cortex, while highest activity was in the occipital and postcentral cortex. The strong enzymic activity in the fronto-polar region was in contrast to the findings of weak activity in the guinea pig.

The gradations of succinic dehydrogenase activity in the upper cortical layers of the guinea pig were paralleled by similar gradations among the thalamic nuclei which project to these regions. This correlation was not as clear-cut in the human brain, since gradations of enzymic activity were less accentuated both in the thalamus and the cortex. The high activity in the fronto-polar cortex was reflected by high activity in the dorso-medial thalamic nucleus, which projects to the fronto-polar cortex.

Allocortex. The pyramidal cells of the fascia dentata (lamina pyramidalis) showed little DPN-diaphorase activity, thus appearing as a light stripe (Figs. 18 and 19). Strong activity was found in the adjacent molecular layer (lamina molecularis) which

was sharply divided into a deep sublamina with weaker activity and an upper sublamina with stronger activity (Fig. 19). The ammonshorn (Fig. 18) showed a band of diffuse enzymic activity in the neuropil and relatively little in the perikarya of the pyramidal cells, except those in Sommer's sector, which showed some activity.

The olfactory bulb (Fig. 17) showed very strong activity in the synaptic glomerula olfactoria, and somewhat weaker activity in the outer plexiforme layer; little reaction was seen in perikarya. This pattern was identical with that in the guinea pig.

DISCUSSION

The present article is mainly of fact-finding nature; the volume and variety of data supplied renders it difficult to provide an adequate discussion. Several implications of chemo-architecture have been discussed in preceding articles on the guinea pig brain (FRIEDE, 1960; 1961*a*, *c*). The present discussion, therefore, is limited to a few general comments.

The purpose of knowledge of chemo-architecture is to help achieve the ultimate goal of understanding all metabolic phases in all regions of the brain. The dimensions of this task limit one either to complete mappings of the distribution of a few enzymes in the entire brain or to broader studies of a spectrum of enzymes in a selected region. Both approaches supplement each other and contribute toward the same goal.

The present data show almost identical patterns of the distribution of DPN-diaphorase, succinic dehydrogenase, and capillarization in the medulla oblongata even though the data were derived from different species and by different techniques. Random material and previous studies indicate a similar distribution of cytochrome oxidase and TPN-diaphorase. This substantiates the assumption that the patterns described demonstrate general gradations of tissue oxidation and energy metabolism, including particularly the citric acid cycle. With this baseline available, one can go on to compare in detail the patterns of enzymes involved in more specific metabolic phases such as the glucose-shunt, or the transmitter-substances.

Even at the present state of knowledge one can benefit from the application of these data to problems of neuropathology. A mapping of the deposition of lipofuscin in the nuclei in the aging human brain showed its extent to be proportional to the normal regional gradations of oxidative enzymic activity (FRIEDE, 1961*d*). This was considered as an indication that the deposition of lipofuscin, or 'wear-and-tear pigment', was proportional to the regional 'wear and tear', that is, the intensity of the oxidative energy metabolism.

SUMMARY

This article provides a detailed mapping of the distribution of DPN-diaphorase in the human brain with histochemical enzyme techniques. Measurements of the gradations of the histochemical reactions were made by spectrophotometric measurement of the formazan formed. The mapping includes measurements in about 135 regions, a description of the cytological enzyme patterns, and 19 photomicrographs. Comparison with previous data from the cat brain reveals a striking similarity between the distribution of DPN-diaphorase in the human medulla oblongata and of succinic dehydrogenase and capillarization in the cat. The enzyme patterns described evidently reflect general gradations of oxidative energy metabolism.

A tendency towards caudo-cranial differentiation of the chemical architecture of the brain is noted, thalamus and cerebral cortex being the most variable regions.

REFERENCES

BURSTONE M. S. (1958) *J. Histochem. Cytochem.* **7**, 112.
FARBER E., STERNBERG W. H. and DUNLAP C. E. (1956) *J. Histochem. Cytochem.* **4**, 254.
FRIEDE R. L. (1960) *J. Neurochem.* **5**, 156.
FRIEDE R. L. (1961*a*) *J. Neurochem.* **6**, 190.
FRIEDE R. L. (1961*b*) *J. Neurochem.* **8**, 17.
FRIEDE R. L. (1961*c*) *Histochemical Atlas of Tissue Oxidation in the Brain Stem of the Cat.* Karger, New York.
FRIEDE R. L. (1961*d*) *Proceedings* IVth *Internat. Congr. Neuropath.* Thieme, 1962.
NACHLASS M. M., TSOU K. C., SOUZA E., CHENG C. S. and SELIGMAN A. M. (1957) *J. Histochem. Cytochem.* **5**, 420.
OLSZEWSKI J. and BAXTER D. (1954) *Cytoarchitecture of the Human Brain Stem.* J. P. Lippincott, Philadelphia.
SCARPELLI D. G., HESS R. and PEARSE A. G. E. (1958) *J. Histochem. Cytochem.* **6**, 369.
SHELTON E. and RICE M. E. (1957) *J. nat. Cancer Inst.* **18**, 117.